Investigation of Quartz Tuning Fork's Dimensional Impact on its Dynamics and Resonance Frequency

Author

Sajid Parveez

00000172262

Supervisor

Dr. Danish Hussain

DEPARTMENT OF MECHATRONICS ENGINEERING

COLLEGE OF ELECTRICAL & MECHANICAL ENGINEERING

NATIONAL UNIVERSITY OF SCIENCES AND TECHNOLOGY

ISLAMABAD

June, 2019

Investigation of Quartz Tuning Fork's Dimensional Impact on its Dynamics and Resonance Frequency

Author

SAJID PARVEEZ

00000172262

A thesis submitted in partial fulfillment of the requirements for the degree of

MS Mechatronics Engineering

Thesis Supervisor:

DR. DANISH HUSSAIN

Thesis Supervisor's Signature: _____

Thesis Co-Supervisor:

DR. MUHAMMAD MUBASHER SALEEM

Thesis Co-Supervisor's Signature: _____

DEPARTMENT OF MECHATRONICS ENGINEERING

COLLEGE OF ELECTRICAL & MECHANICAL ENGINEERING

NATIONAL UNIVERSITY OF SCIENCES AND TECHNOLOGY, ISLAMABAD

June, 2019

Declaration

I certify that this research work titled "*Investigation of Quartz Tuning Fork's Dimensional Impact on its Dynamics and Resonance Frequency"* is my own work. The work has not been presented elsewhere for assessment. I have properly acknowledged / referred the material that has been used from other sources.

Signature of Student

Sajid Parveez

00000172262

Language Correctness Certificate

This thesis has been read by an English expert and is free of typing, syntax, semantic, grammatical and spelling mistakes. Thesis is also according to the format given by the university.

Signature of Student

Sajid Parveez

00000172262

Signature of Supervisor

Copyright Statement

Acknowledgements

First and foremost, I am extremely grateful for special blessings of Allah Almighty upon me throughout my journey. Without which I would never be able to achieve and accomplish what I have today.

A special thanks to my supervisor Dr. Danish Hussain for his great help and constant curiosity about the challenges which I confronted and his cooperative and supportive notions and ideas gave me the direction to successfully and effectively complete my research. I wouldn't be here today without his encouragement throughout the final stages of this research.

I would like to express special gratitude to my co-supervisor Dr. Muhammad Mubasher Saleem for his exemplary supervision, unparalleled insight, and constant encouragement during the course of this thesis.

I would also like to thank Mr. Usman Asad and my G.E.C members Dr. Waqar Shahid and Dr. Amir Hamza for being on my thesis guidance and cordial support at numerous stages which helped me in timely completing of this task.

Finally, I would like to thank my family and friends who have always been an unceasing source of adoration, support and motivation for me.

This work is dedicated to my beloved parents and adored siblings whose tremendous support and encourage enable me to do this wonderful accomplishment

Abstract

The quartz tuning fork (QTF) is an excellent mechanical resonator consisting of two prongs. It is widely used as a time keeping element in watches and telecommunication industry due to its high frequency stability. Tuning fork has wide spectrum of applications for example Atomic Force Microscopy (AFM), near-field scanning optical microscopy (NSOM) and sensors like density, gas, pressure and viscosity sensor, biological sensor and quartz-enhanced photoacoustic spectroscopy (QEPAS). For using QTF as a force sensor in atomic force microscopy, high quality (Q) factor, high force sensitivity and relatively low spring constant are desirable properties. The dimension of quartz tuning fork influences the eigenfrequencies, effective spring constant (k_{eff}) and sensitivity of the quartz tuning fork. We have investigated the dimensional and geometrical impact on eigenfrequencies, effective spring constant (k_{eff}) and sensitivity using analytical and simulation methods. The aim of study is to obtain an optimal design for the QTF having cantilever beam as the basic element with flexible base and enhanced sensitivity. The simulation and analytical results suggest that by reducing the coupling spring constant (k_c) of tuning fork, the effective spring constant (k_{eff}) can be reduce while the sensitivity of tuning fork can be enhanced.

Key Words: *Quartz tuning fork (QTF), spring constant, support loss, sensitivity, Atomic force microscopy (AFM), normal forces, lateral force.*

Table of Contents

List of Figures

List of Tables

Acronyms

MEMS	Microelectromechanical Systems
NEMS	Nanoelectromechanical Systems
QTF	Quartz Tuning Fork
AFM	Atomic Force Microscopy
QEPAS	Quartz-enhanced photoacoustic spectroscopy
NSOM	Near-field scanning optical microscopy
FEM	Finite Element Method

Chapter 1: Introduction

1.1 Introduction

Nanoelectromechanical systems (NEMS) is a field where devices are made having both the electrical & mechanical functional capability at the nanoscale. NEMS is the next advance field of electromechanical system (MEMS). NEMS devices are made by using transistor such as nanoelectronics with mechanical actuators and build to construct the biological, chemical, and physical sensors. As NEMS minute are devices, they are of small mass, minimum power consumption and stable mechanical resonance frequencies are useful in many applications such as in clocks and watches, communication, nanoscale manipulation system. This technology has boost up different field like sensors, instrumentation, biomedical, optical.

In the field of NEMS, Quartz Tuning Fork (QTF) is an excellent mechanical oscillator consisting of two tines. Over the last three decades, as a force sensor the application of quartz tuning fork (QTF) in atomic force microscopy has increased, tremendously. For example, sidewalls imaging [1], surface profile measurements [2] and characterization of intermolecular bonds [3, 4], fast imaging and selective nanorobotics manipulations and stiffness measurement of micro-membrane [5, 6].

Different application of quartz tuning fork (QTF), requires specific optimized parameters such as geometry, crystal cut, quality (Q) factor, eigenfrequency and spring constant. For example, time keeping applications require stable eigenfrequency and atomic force microscopy applications need lower stiffness and higher sensitivity.

In the literature, it has been study that numerous parameters like damping characteristics, material symmetry, support losses and thermoelastic damping can be optimized to enhance the desirable characteristics of the QTF for AFM applications [7]. Hao et al. investigated the geometric properties to give better solution for modelling miniature quartz tuning fork with high working efficiency [8]. Patimisco et al. have modelled different set of QTFs and present the optimized design for optoacoustic gas sensing [9]. There are many factors which contributes to damping losses for example medium surrounding the tines [10], support and anchor [11], thermoelastic [12] and surface of tines [13]. Support is one of main contributing factor to damping loss that effect the TF sensitivity and quality (Q) factor. The tuning fork with coupled tines has higher quality (Q)

factor than single cantilever beam. When single cantilever beam is made to oscillate at specified frequency, the energy waves induced in beam propagates to the fixed and stiff support causing high energy loss as well as attenuation in quality (Q) factor [11]. In quartz tuning fork with two identical prongs, the generated energy waves in both prongs moves toward support and mostly utilized for vibration of each tines through base which acts like coupling spring. Therefore, coupling between tines which acts like spring constant are highly important for reducing damping losses in the tuning fork. Over the last three decades, application of quartz tuning fork as a force sensor in atomic force microscopy has increased, tremendously. For using QTF as a force sensor, high quality (Q) factor, high force sensitivity and relatively low spring constant are desirable properties.

There are various techniques that have been used to calculate the spring constants of QTF. Among these, one of the familiar methods is to find the dimensions of cantilever beam and then calculate the spring constant theoretically. The spring constant changes with variation in the length and thickness, so the inaccurate measurement causes the large error in spring constant value. The large error is because of the thickness measurement. The eigenfrequency measurement can be used to get the estimate value of thickness, which may help to reduce the error.

In other method, if spring constant of one tine is determined accurately. Then, this can be then used to apply known forces to another tine and calibrate them. Repeatably, this is complex method to calibrate the other cantilever. There is another technique that used the intrinsic thermal noise of the cantilever beam. The Brownian motion of any spring-mass system which has proportional expectation value to the temperature and one over the spring constant. The spring constant can be subtracted from thermomechanical displacement measurement and the temperature. The difficulty of this method is to accurately calculate the minute thermomechanical motion over the wide range frequency.

In this thesis, we have designed new tuning fork with flexible base where parallel hinges of quartz act as coupling spring in the middle of both tines and find the spring constant and TF sensitivity by simple method using eigenfrequencies.

1.2 Quartz Tuning Fork

The quartz tuning fork is an excellent mechanical oscillator. This was invented by British trumpeter john shore. The quartz tuning fork is the acoustic oscillator with the U-shaped form that consist on two prongs. The Quartz tuning fork was invented for frequency control. It has stable and precise frequency, and small power consumption. Due to this; they are used as basic component for watches, digital electronics and frequency measurements etc. For example, since 1960s, watches that was built with spring or mechanical pendulum as basic component have been replace by crystal watches. As the results, the quartz crystal resonators take over the wristwatch market.

1.2.1 Basic Working Principle of QTF

When an electric field is applied to quartz tuning fork, then it oscillates at constant frequencies that depends on length and mass of its two prongs. TF continuously generate very stable oscillation frequencies. Electric signals derived from these frequencies are used in electric circuits of many kinds.

In the application such as digital electronics it is used convert electrical energy to precise mechanical and electrical frequencies. In the sensing application, used to convert mechanical or electrical perturbation into a measurable electrical signal. When two prongs of the tuning fork oscillate as a mirror fashion called its fundamental mode. In this mode, the center mass remains stationary and all the forces are counterbalanced within the material coupling the two prongs as depicted in figure 1.1.

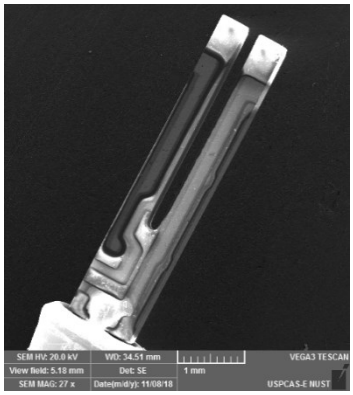

Figure 1.1: SEM image of quartz tuning fork (QTF).

1.2.2 The Tuning Fork with Piezoelectric Effect

The Quartz is one of the materials that has piezoelectrical properties. When mechanical stresses are applied on this type of material then they develop electrical potential. With this effect, it is possible to excite the quartz tuning fork electrically. This material has the lowest intrinsic mechanical losses and the stiffness of quartz give efficient acoustic energy in two prongs of tuning fork due to this QTF's have high quality factors (Q) in the range thousand at fundamental frequency of 32.768 *KHz* in vacuum condition. The quality factor is the essential property to characterize the quartz tuning forks with the application of forces. It is known as the ratio between total energy stored in system and energy dissipated by each oscillation cycle.

1.2.3 The Direct and Inverse Piezoelectric Effect

In direct piezoelectric effect, the quartz material generates the negative and positive charges in portion that is subjected to mechanical stressed. The generated electrical charges are directly proportional to the applied stress. In the inverse effect, the quartz material shows some deformation, when the electric fields are applied to this material.

Let us, consider the slab of quartz material having small thickness compared to the other dimensions. This slab is subjected to the pressure parallel to thickness. By applying the compressional force F, the induced polarization P will be directly proportional to the stress (F/A) as depicted in Figure 1.2. As the results, the piezoelectric polarization produces the charges on electrodes which are laying on the surface and leads to generates the strain gradient. On the application of tensile force, the pressure sign is changed and the polarization reversed.

In the similar way, when the electric field E applied across the plate thickness, the quartz slab show deformation. If the polarity of the field E become reversed, the deformation changes its sign accordingly as described in Figure 1.3.

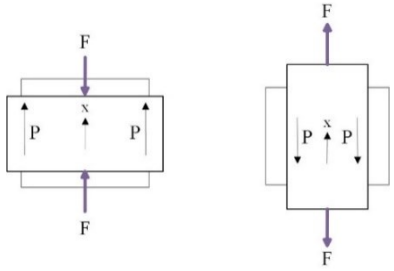

Figure 1.2: Illustrates the direct piezoelectric effect.

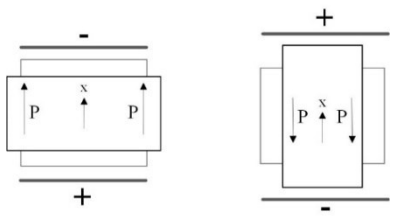

Figure 1.3: Describes the inverse piezoelectric effect

1.2.4 Vibrational Modes of QTF

The tuning fork can serve as the illustration of how a vibrating beam can behave. When the quartz tuning fork is made to vibrate, it shows some vibrational modes. These vibrational modes are describes as following.

a) Fundamental Mode:

In this mode, the two tines of the tuning fork move toward and away from each other, alternately. These shows bending like a fixed-free cantilever beam. As the two prongs moves in the way of mirror image of each other, it is also known as symmetric mode and antiphase mode. This is a basic mode of tuning fork and mostly consider in atomic force microscopy (AFM) [14].

b) Clang Mode:

The second mode shape called clang mode. In this mode, the cantilever exhibit bending in the middle of it. Its frequency is higher than fundamental mode. This also known as symmetric mode.

c) In-plane bending modes:

In this mode, the whole tuning fork vibrates as one object, instead of vibrating as separate cantilever. This also called asymmetric mode and inphase mode.

d) Out-of-plane bending mode:

Here, the tuning fork behaves like solid bar and oscillate normal to the plane of tines. But in the asymmetric out of plane mode, the two tines oscillate normal to the tuning fork plane but in different directions.

1.2.5 Application of Quartz Tuning fork

The quartz tuning fork has diverse application areas due to its high stable and precise frequency, low cost, miniature size and small power consumption.

a) In Musical Instruments

The forks have been used for tuning the musical instrument [15, 16]. Tuning forks like structure used in Rhodes Piano to generate sound. Electric amplifier is used to amplify the generated sound. Piano has hammer hitting like constructions that work on same principal as tuning forks.

b) In Clocks and Watches

Crystal oscillator used as the time keeping element in modern clocks and watches as depicted in Figure 1.4. This is an electric circuit that utilizes the mechanical oscillating crystal to generate electrical signal having precise frequency. Then, this frequency is used for time keeping [17].

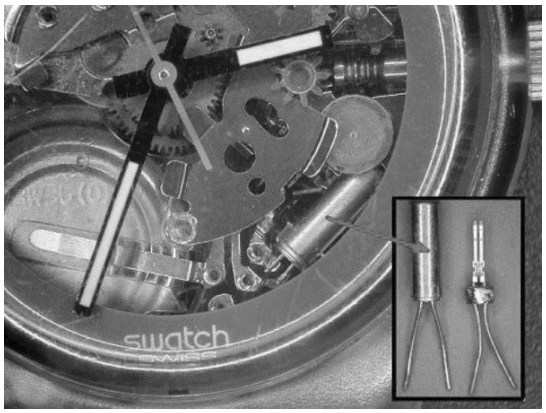

Figure 1.4: Shows the use of QTF as an oscillator in Swatch^{TM} watch [18].

c) Medical Uses

Medically, The doctors used the tuning fork to assess a patient's hearing [19]. This is done with two exams like weber test and Rinne test. In Weber test, the tuning fork (512 *Hz*) is brought close to the forehead of patient. If sound is higher on one side than the other side, this manifest that patents may have middle ear or inner ear hearing loss. In Rinne test, same tuning fork is press against the mastoid bone and then brought close to ear canal. if sound is louder in AC than in BC then this test is positive.

d) Electronics Circuits

As stable frequency device, electric signals derived from tuning forks are used in electric circuits of radios, televisions, mobile phones, computer processor and other devices that rely on wireless signals [20-23]. These devices are unable to send or receive information because they work on the specific designed frequency.

e) SEM Nanorobotics Manipulation System

In the SEM, tuning fork used as force sensor. This is a used determine mechanical property of minute structures (like tiny wires, carbon tubes, membranes etc.) [24]. This system is composed of two nanomanipulator and TF is fixed between these manipulator as depicted in Figure1.5. This system discloses the stiffness of nanostructures when they are elongated with controlled tensile force. With the help of Hooke's, law stiffness can be transformed into forces.

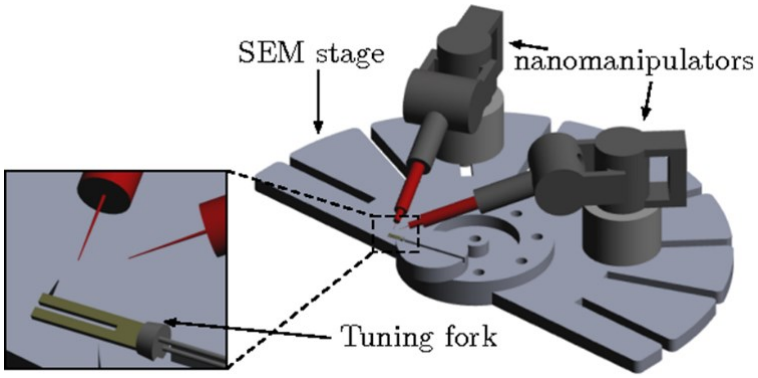

Figure 1.5: Nanorobotic manipulation system [25].

f) Industrial Process Control

In industrial tuning fork level switch is used to maintain liquid level in tank. The excited tuning fork to its resonance frequency, when submerged into the liquid. The variation in resonance frequency is traced to find liquid level [26].

1.3 Losses in Quartz Tuning Fork

The most important parameter of mechanical resonator like tuning fork is quality factor. Higher the quality factor, lower the energy losses as compare to the stored energy. With high quality factor, frequency of the resonator will be sharp. This characterize the bandwidth of fork with respect to its center frequency. The following type of losses are found in quartz tuning fork mainly.

a) Air damping
b) Support and Anchor loss
c) Thermoelastic damping
d) Surface loss

When tuning fork tines vibrate, the surrounding medium like air interact with its tines and cause to loss of energy [10]. With the increase of air pressure, the air damping will increase respectively. The vibrational energy wave propagates to the support. The high stiffness of support causes to loss of energy.

When tuning fork vibrates, its tines deformed causes to induced strain field. This leads to generate the temperature gradient and thus energy loss due to increase in entropy. This phenomenon known as thermoelastic damping explained by Zener [12], for the cantilever beam of rectangular cross-section.

The surface losses contributes to the tuning fork damping [13]. The surface to volume ratio increases for the miniaturized tuning fork. At the surface of tuning fork there may be impurities, lattice defects and imperfection. These manifest that the surface effects become significant and leads to loss of energy. The total quality factor is defined with the contribution of all these sources is given, as in [13].

$$\frac{1}{Q_{total}} = \frac{1}{Q_{air}} + \frac{1}{Q_{TED\ dissipation}} + \frac{1}{Q_{support}} + \frac{1}{Q_{surface}} \qquad (1.1)$$

1.4 Why QTF is Used in AFM rather than Simple Quartz Cantilever Beam

Upon the simple cantilever, the quartz tuning fork has following advantages: -

a) A simple quartz cantilever can be used but unlike this under the same condition QTF gives high Q-factor than simple beam.
b) This leads to improved sensitivity of tuning fork.
c) The tuning fork is of two coupled cantilever beam resonating in mirror fashion. The center mass remains still, regardless of its prong's vibration. Unlike the vibration of simple cantilever beam having resonating center mass.
d) These vibration results in reduction of Q-factor and dissipates energy. In the symmetric tuning fork this type energy dissipation is not present. Only internal energy dissipation and emission of acoustic waves exist. Hence overall energy dissipation reduces.

It has been shown that the quartz tuning fork is better than simple cantilever beam and can be deployed as force sensor with high advantage in Atomic Force Microscopy (AFM).

1.5 Application of QTF in Atomic Force Microscopy (AFM)

When the Scanning Tunneling Microscope (STM) was invented [27, 28], the Scanning Probe Microscopy (SPM) has become indispensable technique for researcher to investigate the physics at nanometer scale [29-32]. For the first time, this invention enables the researcher to take the high resolution image of individual atom. The working principle of STM was based on tunneling current. This current produced by conductive probe when it is close to the conductive surface having different potential from probe. The tunneling current amplitude leans on the distance between tip and surface of the sample. In the STM, the scanning probe is fixed on scanning device and the voltage is supplied between surface and probe. The scanning probe brought close to surface. When the distance between the probe and sample of surface reaches to few Angstroms, the tunneling current induced between them. The topographic image is acquired by the movement of scanning device. But the working principle of STM limits its uses because it requires both the tip and surface to be conductive.

To acquire the topography image of non-conductive surface, the interaction forces was considered instead of tunneling current between them. When the STM was invented after the few years, this led to the development of first atomic force microscopy in 1986 [33-35]. Many types

of scanning probe microscopy have been developed like Magnetic Force Microscopy (MFM) [36], Electrostatic Force Microscopy (EFM) [37] and Near Field Scanning Optical Microscopy (NSOM) [38]. All of these have a common characteristic as in STM: they used probe for sample scanning and then interaction between probe & surface serve as feedback to control the separation between the surface of selected sample and tip. The big difference in atomic force microscopy and other technologies is that the atomic force microscopy (AFM) does not depend on the use of lenses or beam irradiation. That's why, it does not face restriction in spatial resolution as the result of aberration and diffraction and making a room to controlling the cantilever beam (by building vacuum) and no need to dying the sample.

For the enhancement in resolution, force sensor with improved sensitivity are required. For this purpose, many types of micro-machined cantilever beam have been deployed to detect the mechanical, thermal, electrical and magnetic property. Due to high quality (Q) factor, the quartz tuning fork was deployed in scanning probe microscopy. According to principles, all of the scanning probe microscopy (SPM) depends on the interaction within the tip and sample surface of diverse materials. Difference between scanning probe microscopy and other technologies are the way of tip and sample interaction and technique by which interaction is monitor. For example, in the electrostatic force microscopy, the forces are determined within tip and sample surface that produces due to potential difference. But in the atomic force microscopy (AFM), all types of forces can be determined between tip and sample including long range forces like magnetic and electrostatic forces and short-distance forces like van der Waals and attraction forces within atoms.

1.5.1 Basic Working Principle of AFM

It became practical to take high resolution image of conductive and insulating surface by the invention of Atomic Force Microscopy (AFM) [39-41]. Atomic Force Microscopy (AFM) is the kind of scanning probe microscopy (SPM). The AFM has ability to observe all of the interactions between tip and sample surface. These interactions are type of forces such as chemical force, van der Waals force, electrostatic force and magnetic force that lean on the distance between tip & sample surface and also on the material properties [42, 43]. The AFM is a most important technique that is used to determine the intermolecular force experimentally.

To monitor the intermolecular force, a tip is fixed at the free end of cantilever and used as a force sensor. When it reaches to the surface of sample observing, then it will face an interactive

force. Due to this force, the cantilever beam exhibits some bending. To track the bending or the oscillation of the cantilever, it requires the detection system. The laser beam is the most familiar system as shown in Figure 1.6 (A). It is employed to monitor the deflection of the cantilever. In his working, the laser beam is directed to surface of cantilever and then this reflected to a quadrant photodiode. The photodiode is set in such a way that the laser beam reach to the center of photodiode when the cantilever beam experiences no interaction force. As the tip come close to the sample surface, interaction force tends to bend the cantilever beam up or down depending on the intensity of the force between tip and sample surface. The photodiode detects the bending and torsion in cantilever beam, then send the deflection value toward feedback controller. In this way, the interaction force can be determined quantitively. During the scanning of sample surface by tip, the feedback controller adjusts the height position of surface to keep constant the photodiode signal. Thus, topography of sample surface can be mapped by recording the height position.

The AFM has the superiority to acquire images of various type of surface, such as composite materials, biological samples, polymers, ceramics and glass. AFM have two basic modes as describe in Figure 1.6 (B). Contact mode (where tip makes direct contact to surface) and non-contact mode (where the cantilever vibrates near to the sample).

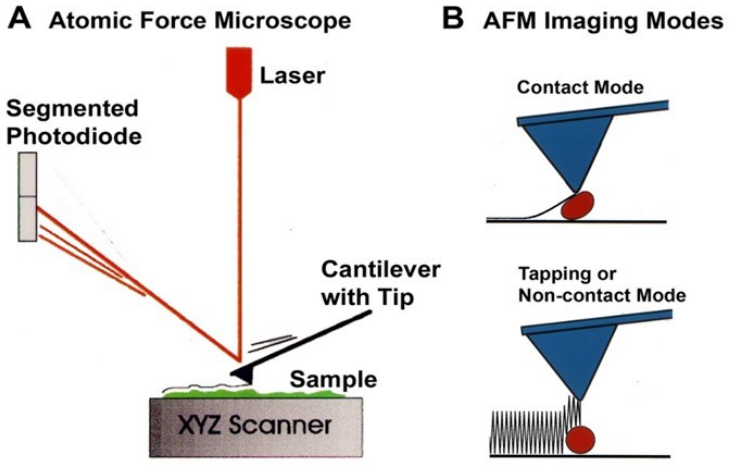

Figure 1.6: Depicts the working of atomic force microscopy (AFM) [18].

Because the atomic force microscopy depends on the forces between tip & the surface of sample, these forces highly influence the imaging process. The force-distance is illustrated in Figure 1.7.

If tip is in hard contact to the sample surface, then the interaction forces are repulsive.
If the tip and surface of sample have small distance between them, then there will be attractive forces.
If the tip and surface of sample have large distance between them then there will be no force gradient, no deflection.

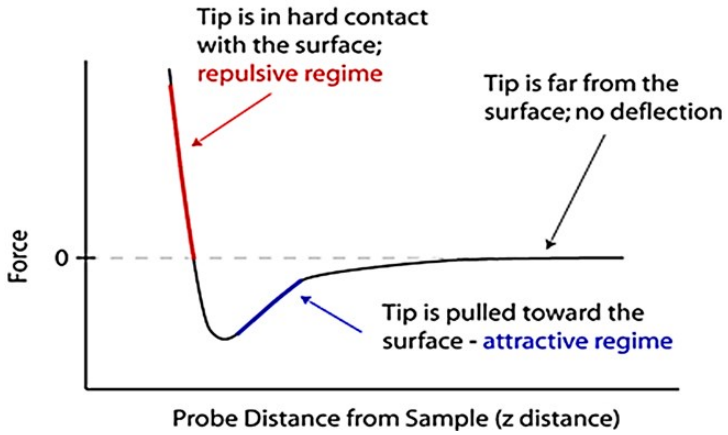

Figure 1.7: Describes the force-distance of atomic force microscopy [18].

1.5.2 Dynamics Modes of AFM

These are the collection of Atomic Microscopy scanning modes in which the cantilever beam vibrates at specified frequencies or resonance frequency as describe in Figure 1.8. The different materials of sample have different properties like chemical composition that results in different rigidity, electric polarity and chemical property. In order to optimize the determination of the interaction force for diverse sample material, there is different scanning modes of Atomic Force Microscopy (AFM). The four familiar scanning modes of AFM are following.

a) First Mode

The first scanning mode is known as contact mode as depicts in Figure 1.8 (a). In this mode, tip glued at free end physically touches the sample surface. This mode is commonly used for rigid samples. Its scanning speed is quite fast and operate in repulsive interactive regime. But during scanning the surface, the tip may damage quickly.

b) Second Mode

The second scanning mode is called non-contact as illustrated in Figure 1.8 (b). In this mode, the cantilever beam vibrates at natural frequency due to the external dither. The drop in vibrational amplitude and phase changes because of interaction forces between the tip and sample. To take the topography image of sample surface, it is necessary to keep vibration amplitude at constant level by using feedback controller and tip operate in the attractive regime. In the 2^{nd} mode, tip does not touch the surface and has relatively lower amplitude. This mode is used for scanning the soft, fragile sample surfaces. As the tip never touch the surface of sample, this thing ensures the safety of tip during scanning. But some details on sample may left undetected.

c) Third Mode

This mode is familiar as tapping mode as illustrated in Figure 1.8 (c). Its working principle is same as of the non-contact mode. In the mode, tip not only able to operate in attractive regime but it also works in repulsive regime and having relatively large vibrational amplitude. This is the only thing that distinguishes the tapping mode from non-contact mode. Periodically, tip touches the sample surface.

d) Fourth Mode

The fourth mode is called jumping mode as shown in Figure 1.8 (d). This mode is similar to contact mode but tip does not damage the sample surface. In the mode, the cantilever beam does not tend to vibrate. For properly scanning the surface, distance within tip and sample surface vs force curve is drawn [44]. In the start, the tip is far from the sample surface then brought closer until the interaction forces meets the specified set point. But the force vs tip and surface distance curve, for each scanning position lowers the scanning speed significantly. This is the only disadvantage.

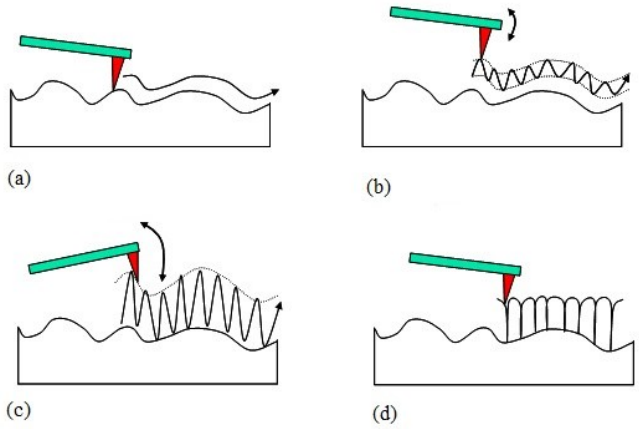

Figure 1.8: Describe different modes of AFM. (a) Contact mode. (b) Non- contact mode. (c) Tapping mode. (d) Jumping mode [18].

1.5.3 Abilities of Atomic Force Microscopy (AFM)

It has following abilities

1) Measurement of forces
2) Topography imaging
3) Manipulation ability

For the measurement of forces, it can be utilized to determine the forces within surface of sample and tip [45, 46]. AFM can be deployed to perform the force spectroscopy, determine the mechanical properties of the sample likes Young's modulus (*E*), stiffness, adhesion strength etc.

For imaging, the AFM can be utilized to acquire the topography image surface of sample under observation. With the help of these forces, it is possible to form an 3D image at higher resolution [47, 48]. It is done by obtaining the position of the sample with help of the raster scanning, w.r.t the attached tip and recording the probe height. Then surface topography image is shown by pseudo color plot.

For the manipulation, these forces can also be employed to varies the properties of the sample with the help of controlled technique [49, 50]. For instance, manipulation at atomic level, scanning probe lithography and locally stimulation of cells.

1.5.4 Application of AFM

To solved problems in diverse range of discipline in natural sciences, the atomic force microscopy has been utilized, such as

a) Topography Imaging

For imaging, the interaction of force within the tip and surface of sample can be employed to form the topography image of surface profile with high resolution. The atomic force microscopy has capable to obtain image of almost any kind of sample surface including conductive and isolating surfaces.

b) Force Measurements

The atomic force microscopy (AFM) has been employed to determine the force vs distance curves. These curves explain the interaction of force exist within the tip and sample surface.

c) Characterization of Material Properties

The material properties can be determined with the help of AFM. To extract different properties of sample material, the forces distance curves is determined. These curves give valuable information about elasticity, hardness, adhesion and surface charge densities etc.

d) AFM Manipulations

The manipulations of atoms and molecules on surfaces, serves as the model of construction and characterization of system. The atomic force microscopy (AFM) is capable for investigation of variations in physical properties because of variations in an atomic ordering by manipulation.

e) Molecular biology

Application of molecular biology include, the atomic force microscopy can be utilized to investigate the structural and mechanical properties of protein [51]. For example, AFM has been used to obtain the topography profile of microtubules and determine its stiffness.

f) Cell Biology

In the cellular biology, atomic force microscopy is utilize to identify the cancer cells and normal cells based on a their stiffness and to study interaction within a specific cell and next nearby cells [52].

g) Medical field

The AFM techniques have been utilizing in the field of Medical and Pharmacological Applications. For instance, Enzyme hydrolysis visualizations are carried out by phase imaging mode of atomic force microscopy [53], The capability to scan the interaction between SLBs (supported lipid bi-layers) and drug [54, 55]. For the dental application, the AFM is used to investigate gutta-percha cone topography and it offer a new technique to evaluate the characterization of the gutta-percha cone surfaces directly [56].

1.6 Conclusion

In this chapter, an introduction to quartz tuning fork (QTF) and atomic force microscopy (AFM) is presented while describing their different types and diverse applications. It is described that how spring constant is computed with different technique in previous research. It is briefly explained that why quartz tuning fork has better use over simple cantilever beam. Also, the advantages of the AFM over other related fields is discussed. Then, the comprehensive literature review of the prior research carried out on quartz tuning fork (QTF) dimensional impact on its dynamics and eigenfrequencies is presented.

Chapter 2: Proposed Design of Quartz Tuning Fork

The objective of any type of sensor is to measure a specific signal on real time in existence of noise. The sensor that give large response to the small interaction between tip and sample surface is consider as better performance of sensor and is known as sensor sensitivity. In this chapter, we have proposed a novel design of quartz tuning fork with flexible base to enhance the sensitivity of tuning fork and discussed the important parameters of tuning fork.

2.1 Important parameters of Tuning Fork

There are following important parameter for quartz tuning fork having cantilever beam as basic element.

1) Sensitivity
2) Spring Constant
3) Noise
4) Resolution

2.1.1 Sensitivity

The sensor that give large response to the small interaction between tip and sample surface is consider the measure of sensor sensitivity. The sensitivity of tuning fork depends on spring constant and its antiphase frequency. For force sensor, the sensitivity is measure in volts per Newton (V/N) and for displacement sensor it is measure in volts per meter (V/m). For piezo-resistor, the variation in resistance is converted into voltage with the help of Wheatstone bridge.

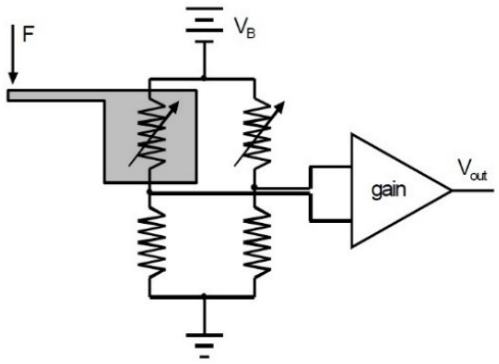

Figure 2.1 Describes the Wheatstone bridge for piezoresistive cantilever beam [57].

From the Figure 2.1, it can be noted that sensitivity can made large by changing the gain of amplifier. Sometime the sensitivity is given as fractional change per signal. For instance, to the variation in resistance of the piezo-resistor force sensor given as $\Delta R/R$ per Newton (N^{-1}).

2.1.2 Spring Constant

The coupling spring constant (k_c) of a cantilever beam is critical, when using it as the sensor. In chapter 5, it will be described that by decreasing the coupling spring constant (k_c) improves the tuning fork force sensitivity. The results suggest that for lower spring constant and enhance sensitivity, the coupling hinges should be of shorter length (l_h) and relatively higher width (w_h) & thickness (t_h) for force measurements. However, there are some restrictions on the cantilever beam spring constant.

However, the soft cantilever beam when using it as force sensor has some disadvantage in the sense of tip stability. The soft cantilever with spring constant (k) less than 15 pN/0.34 nm = 0.04 N/m has tip instability issue. These instabilities issues occur when the attractive force gradient between tip and sample surface exceeds the cantilever spring constant and it will be stationary when the attractive force equals the spring constant.

For contact AFM imaging, the cantilever beam with higher spring constant exert relatively large force on sample surface and it may damage the surface as well as tip may undergoes to wear. Therefore, the acceptable spring constant for imaging solid surface should be in range of 1-10 nano-Newton (nN) and for imaging biological sample surface, it should be less than ~0.1 nN.

2.1.3 Noise

Without any input, the output signal is called noise. For circuit given in Figure 2.1, when there is no input force signal given to the cantilever beam, any output voltage V_{out} induced is known as noise. If the frequencies contain some noise that causes an error in measurement, in order to improve the signal to noise ratio, they can be filtered by electronically.

2.1.4 Resolution

The minimum force that can be measure by probe is known as its resolution. It can also be stated as noise divided by sensitivity. The total noise depends on the bandwidth, since electronic

filters eliminate the noise that are outside of bandwidth. The resolution can be stated as the minimum measurable force in particular bandwidth and given as *N/ Hz* for measurements in a 1 *Hz* bandwidth.

To enhance sensor performance, there are varies parameters like drift, dynamic range, linearity and accuracy. Dynamic range and linearity are not used for atomic force microscopy (AFM) sensors, as the probes has feedback mode where the main objective is to maintain the constant force on the cantilever beam.

2.2 Quartz Tuning Fork Design

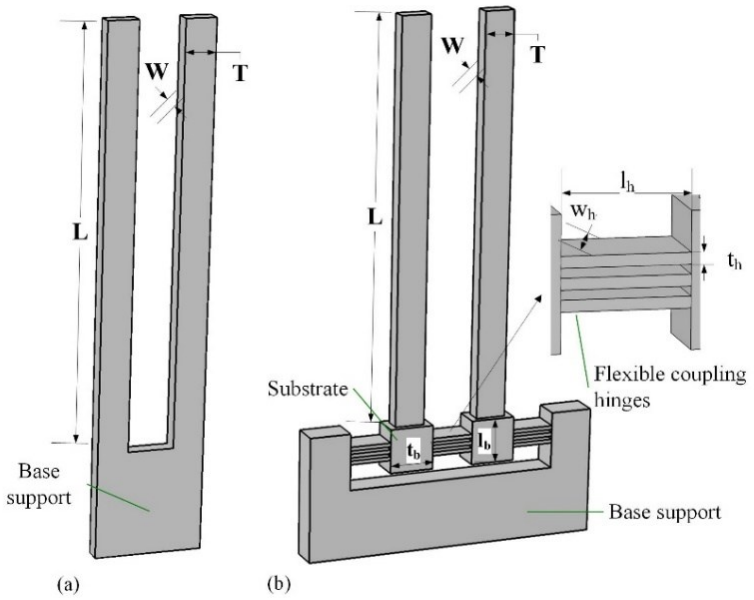

Figure 2.2: (a) Standard Quartz Tuning Fork. (b) Schematic view of proposed design QTF.

To investigate the impact of inter tine coupling spring constant (k_c), we propose a new design of inter-tine coupling with flexible base for QTF as shown in Figure 2.2 (b). The Figure 2.2 (a) is the standard model of tuning fork with higher coupling spring constant (k_c). The has lower sensitivity due to its high spring constant. In the new design, each tines of tuning fork are anchored to substrate and suspended at the support with flexure hinges. The set of three parallel hinges are used to attach the substrate with each other and to the fixed base support. The proposed design prioritizes the stiffness tuning of coupled oscillator through mechanical design for enhanced sensitivity.

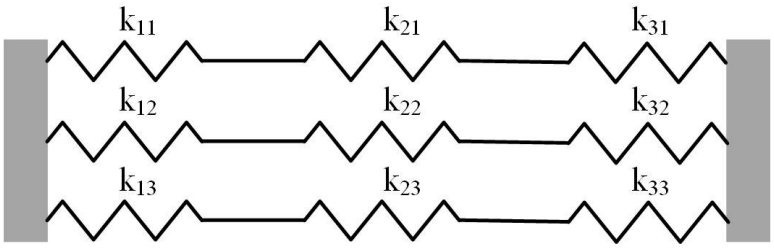

Figure 2.3 Schematic diagram of spring system illustrating series and parallel combination of springs.

To calculate the equivalent spring constant (K_{eq}), the hinges are combined using adequate spring system as shown in Figure 2.2. The rigid substrate has stiffness much larger than that of hinges.

For parallel hinges

$$\begin{aligned} k_{eq1} &= k_{11} + k_{12} + k_{13} \\ k_{eq2} &= k_{21} + k_{22} + k_{23} \\ k_{eq3} &= k_{31} + k_{32} + k_{33} \end{aligned} \tag{2.1}$$

Then combing in series, yields

$$\begin{aligned} \frac{1}{K_{eq}} &= \frac{1}{k_{eq1}} + \frac{1}{k_{eq2}} + \frac{1}{k_{eq3}} \\ K_{eq} &= \frac{k_{eq1}.k_{eq2}.k_{eq3}}{k_{eq2}.k_{eq3} + k_{eq1}.k_{eq3} + k_{eq1}.k_{eq2}} \end{aligned} \tag{2.2}$$

For simplicity, consider all the hinges are identical. For rectangular cross-sectional hinges, K_{eq} is given, as in [58]

$$K_{eq} = \frac{E w_h {t_h}^3}{12 l_h} \tag{2.3}$$

Where E is the young's modulus (E= 78.7 GPa). The l_h, w_h, and t_h are length, width and thickness of coupling hinges respectively.

2.3 Conclusion

In this chapter, the important design parameters of quartz tuning fork (QTF) are discussed that play a key role in the design of AFM sensors. To design the AFM sensor, these parameters are considered, by changing them the quality of AFM sensor can be enhance. For instance, when

focusing on spring constant of tuning fork. It depends on geometrical dimensions of tines. By variation in dimension, spring constant can be increase or reduces and this significantly increase the sensitivity as well as quality of AFM sensor. This chapter explain the new design of quartz tuning fork on basis of spring constant. The new design is proposed with flexible base to enhance the sensitivity of tuning fork while describing its advantages over the standard model. Then, developed the analytical model using adequate spring system for flexible base.

Chapter 3: Analytical Modelling of Quartz tuning Fork

The quartz tuning fork has been modelled as single cantilever beam using mass-spring system where tines behaves like uncoupled cantilever beams. The coupled harmonics oscillator model is widely accepted because it is well validated with experimental results [59, 60]. Each tine is modelled as a mass spring system with the coupling spring between them as shown in Figure 3.1. As tuning fork behaves like pair of coupled oscillators, its dynamics is influenced by coupling spring between tines. In this chapter, developed the analytical model for single and coupled oscillator while explained the mechanical and electrical model of tuning fork.

3.1 Quartz Tuning Fork Model

The mechanical modeling of quartz tuning fork can be developed by considering single harmonic oscillator and coupled harmonic oscillator using mass spring system. The electrical model of quartz tuning fork (QTF) can be developed by Butterworth and Van Dyke model. The mechanical and electrical model are briefly explained as following: -

3.1.1 Mechanical Model

In the most of research work, mechanical model of tuning fork is developed by using mass-spring system where the coupling within two tines is shown by coupling spring constant. This model is widely accepted due to its valid experimental results.

a) Single Harmonic Oscillator

Quartz tuning forks have been modelled as single cantilever beam in most of research paper [61-63] where tines of tuning fork behaves as uncoupled cantilever beam. The tuning fork is fixed in the holder structure. One arm of tuning fork is considered as vibrating cantilever beam. The equation of motion for fixed-free cantiliver beam can be expressed as follwing

$$m\ddot{x}(t) + b\dot{x} + kx(t) = F(t) \tag{3.1}$$

Where m, b, k are mass, damping and elastic constant of the oscillator system respectively. Static spring constant of rectangular cantilever determined by geometrical properties of tines can

be given by

$$k = \frac{EWT^3}{4L^3} \tag{3.2}$$

E, W, T and L are young's modulus of quartz material, width, thickness and length of cantilever. Symmetry of tuning fork is most important for q-factor. The resonance frequency of balance tuning fork depends on length, cross-sectional geometry of tines and material properties of fork and given by

$$\mathrm{f} = \frac{1}{2\pi}\frac{5t}{2\sqrt{6}l^2}\sqrt{\frac{E}{\rho}} \tag{3.3}$$

ρ is the material density.

b) Coupled Harmonic Oscillator

The coupled harmonics oscillator model is widely accepted because it is well validated with experimental results [59, 60]. As tuning fork behaves like pair of coupled oscillators, its dynamics is influenced by coupling spring between tines. The equation of motion of QTF modelled as coupled harmonic oscillator is drive by using Lagrange equation. The identical tines of tuning fork have their effective masses including substrate $m_1 = m_2 = m$ and spring constant $k_1 = k_2 = k$. The coupling between tines is represented by coupling spring constant (k_c) as shown in Figure 3.1. As tuning fork behaves like pair of coupled oscillators, its dynamics is influenced by coupling spring between tines. The equation of motion for coupled oscillator can be expressed as

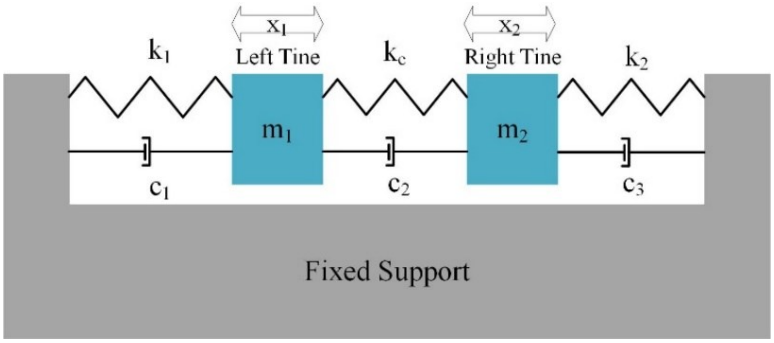

Figure 3.1: Mechanical model of coupled harmonic resonator where x_1 and x_2 represent the position of left and right tines.

The equation of motion for coupled oscillator can be found using Lagrange equation given as.

$$\frac{d}{dt}\left(\frac{\partial P}{\partial \dot{x}_i}\right) - \frac{\partial P}{\partial x_i} + \frac{\partial D}{\partial \dot{x}_i} + \frac{\partial K}{\partial x_i} = F_i \tag{3.4}$$

Where

P, D, K and *f* represents the potential energy, energy dissipation, kinetic energy, and the force function for driving the system respectively. The subscript (*i = 1,2,3*) represent the degrees of freedom DOF.

The potential energy, energy dissipation and kinetic energy are given by the equation (3.5), (3.6) and (3.7).

$$P = \frac{1}{2}m_1\dot{x}_1^2 + \frac{1}{2}m_2\dot{x}_2^2 \tag{3.5}$$

$$K = \frac{1}{2}k_1x_1^2 + \frac{1}{2}k_c(x_1 - x_2)^2 + \frac{1}{2}k_2x_2^2 \tag{3.6}$$

$$D = \frac{1}{2}c_1\dot{x}_1^2 + \frac{1}{2}c_2\dot{x}_2^2 + \frac{1}{2}c_3\dot{x}_3^2 \tag{3.7}$$

By applying the Lagrange equation on (3.5 – 3.7) and, the resultant equations of motion for damped oscillation system are given as follows:

$$\begin{aligned} m_1\ddot{x}_1 + c_1\dot{x}_1 + (k_1 + k_c)x_1 - k_2x_2 &= F_1 \\ m_2\ddot{x}_2 + c_3\dot{x}_2 - k_cx_1 + (k_c + k_3)x_2 &= F_2 \end{aligned} \tag{3.8}$$

For free and undamped system consider *F = 0, C = 0*.

The equation of motion for free and undamped system can be expressed as

$$\begin{aligned} m_1\ddot{x}_1(t) + (k_1 + k_c)x_1(t) - k_cx_2(t) &= 0 \\ m_2\ddot{x}_2(t) - k_cx_1(t) + (k_c + k_2)x_2(t) &= 0 \end{aligned} \tag{3.9}$$

Assuming that the two masses m_1 and m_2 have same harmonic oscillation.

For m_1,

$$x_1(t) = X_1\cos(\omega t + \varphi) \tag{3.10}$$

For m_2,

$$x_2(t) = X_2 \cos(\omega t + \varphi) \tag{3.11}$$

Where $X_1$and X_2 are constant that represent the amplitude of $x_1(t)$ and $x_2(t)$. By substituting Eq. (3.10) & (3.11) into Eq. (3.9), we get

$$\begin{aligned}[\{-m_1\omega^2 + (k_1 + k_c)\}X_1 - k_c X_2]\cos(\omega t + \varphi) = 0\\ [-k_c X_1 + \{-m_2\omega^2 + (k_c + k_2)\}X_2]\cos(\omega t + \varphi) = 0\end{aligned} \tag{3.12}$$

To satisfy theses equation for time t, the terms between the brackets must be equal to zero.

$$\begin{aligned}[\{-m_1\omega^2 + (k_1 + k_c)\}X_1 - k_c X_2] = 0\\ [-k_c X_1 + \{-m_2\omega^2 + (k_c + k_2)\}X_2] = 0\end{aligned} \tag{3.13}$$

For no vibration, these equations satisfy by making $X_1 = X_2 = 0$.

$$\det\begin{bmatrix}\{-m_1\omega^2 + (k_1 + k_c)\} & -k_c \\ -k_c & \{m_2\omega^2 + (k_c + k_2)\}\end{bmatrix} = 0$$

or

$$(m_1 m_2)\omega^4 - \{(k_1 + k_c)m_2 + (k_c + k_2)m_1\}\omega^2 + \{(k_1 + k_c)(k_2 + k_2) - k_2^2\} = 0 \tag{3.14}$$

This is known as the frequency or characteristic equation. The solution of this expression provides frequencies or characteristic values of system.

Thus, roots of Eq. (3.14) are

$$\begin{aligned}\omega_1^2, \omega_2^2 = \frac{1}{2}\left\{\frac{(k_1 + k_c)m_2 + (k_c + k_2)m_1}{m_1 m_2}\right\}\\ \pm\frac{1}{2}\left[\left\{\frac{(k_1 + k_c)m_2 + (k_c + k_2)m_1}{m_1 m_2}\right\}^2 - 4\left\{\frac{(k_1 + k_c)(k_c + k_2) - k_c^2}{m_1 m_2}\right\}\right]^{\frac{1}{2}}\end{aligned} \tag{3.15}$$

The solution for two degrees of freedom mass-spring system in the harmonic oscillation can be given by two eigen modes. One is in-phase in which the whole oscillator acts as single object and the other is anti-phase in which the two tines of the fork vibrates in the mirror fashioned. The anti-phase mode is called fundamental mode. These modes of two similar tines with effective masses ($m = m_1 = m_2$), spring constant of one tine (k) and coupling spring (k_c) between them, are given, as in [64].

$$\omega_{in-phase} = 2\pi f_{in-phase} = \sqrt{\frac{k}{m}}$$

$$\omega_{anti-phase} = 2\pi f_{anti-phase} = \sqrt{\frac{k+2k_c}{m}} \quad (3.16)$$

Where k_c is coupling spring constant of the two identical cantilevers. The coupling spring constant (k_c) can be expressed as.

$$k_c = \frac{k}{2}\left[\left(\frac{f_{anti-phase}}{f_{in-phase}}\right)^2 - 1\right] \quad (3.17)$$

The effective spring constant (k_{eff}) of coupled oscillator can be expressed in term of static spring constant of tuning fork and eigen frequencies ratio as following.

$$k_{eff} = 2k\left(\frac{f_{anti-phase}}{f_{in-phase}}\right)^2 \quad (3.18)$$

Measure of quality factor "Q" depends on the amplitude and frequency response of the tuning fork. The quality factor is dimensionless parameter of oscillator system that measures the energy losses in the vibrating structure.

$$Q = \frac{f_o}{\Delta f} \quad (3.19)$$

Δf is measured at the FWHM of the waveform.

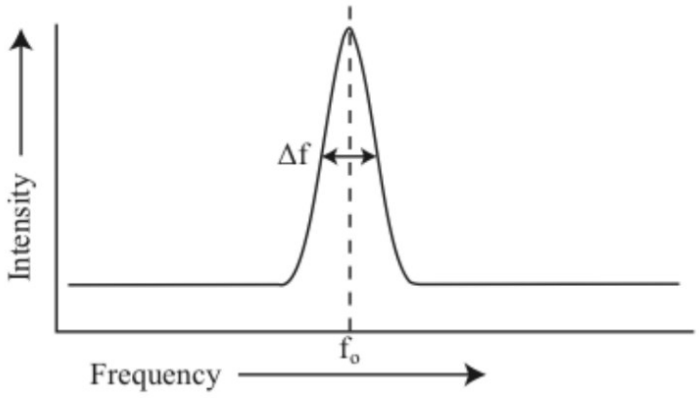

Figure 3.2 Describes the qualitative measure of the Q-factor for resonator by FWHM curve [65].

3.1.2 Electrical Model of QTF

It is possible to excite and detect the oscillation of tuning fork's electrically with the help of electrode laid on the sides of two tines. Starting from the equation of motion for simple harmonic. The tuning fork electrically can be driven by the force $Fcos(\omega t)$ with the application of an AC voltage across the electrodes laid on the fork.

$$m\ddot{x}(t) + b\dot{x} + kx(t) = F\cos(\omega t) \tag{3.20}$$

Due to piezoelectric effect, quartz undergoes to mechanical strain in the presence of electrical field. The displacement of the tines from its original position is proportional to the charge on electrodes.

$$q = Kx \tag{3.21}$$

Where K represents the tuning fork constant.
The alternating current will make the tines to show deflection in oscillatory way.

$$I = K\frac{dx}{dt} \tag{3.22}$$

The driving force can be express in term of amplitude of voltage as

$$F = \frac{K}{2}V \tag{3.23}$$

Substituting the expression for F and $\frac{q}{x}$ for x in the simple harmonic equation and we get

$$\frac{m}{K}\frac{d^2q}{dt^2} + \frac{b}{K}\frac{dq}{dt} + \frac{k}{K}q = \frac{K}{2}V\cos(\omega t) \tag{3.24}$$

This expression has same form as LRC circuit.

$L = \frac{2m}{K^2}$, $R = \frac{2b}{K^2}$, $C = \frac{K^2}{2k}$

Where

L is for inductance that is used for size of kinetic energy storage. (i.e., effective mass)

R is for resistance that models the dissipative processes.

C is for capacitor that shows potential energy storage. (i.e., the spring constant)

This equivalence between piezoelectric resonator and LRC circuit can be expressed by Butterworth and Van Dyke model is shown in Figure 3.3.

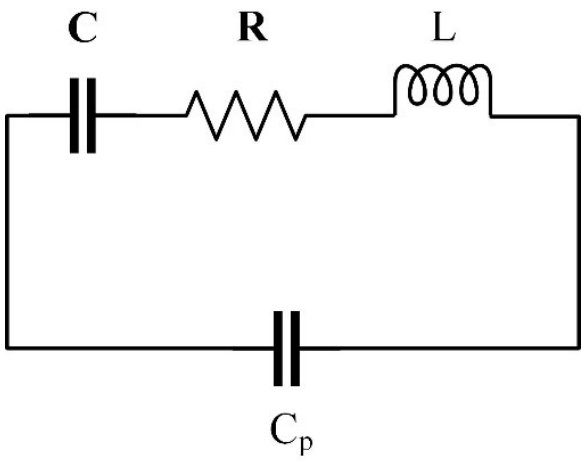

Figure 3.3: Schematic view of electrical model.

Here C_p represent parasitic capacitance of circuit involving QTF. It depends on length and types of cables used.

3.2 Conclusion

In this chapter, the mechanical and electrical model for single and coupled oscillator are described. The quartz tuning fork has been modelled as single cantilever beam using mass-spring system where tines behaves like uncoupled cantilever beams. The coupled harmonics oscillator model is widely accepted because it is well validated with experimental results and then developed the equations of motion using Lagrange equation and derived the analytical equation for eigenfrequencies, coupling spring constant (k_c), effective spring constant (k_{eff}) and TF sensitivity. Each tine of quartz tuning forks is modelled as a mass spring system with the coupling spring between them. As tuning fork behaves like pair of coupled oscillators, its dynamics is influenced by coupling spring between tines.

Chapter 4: Finite Element Analysis of QTF

In this Chapter, a comprehensive FEM based simulation methodology is discussed for the proposed quartz tuning fork (QTF). Finite Element Analysis is important to simulate the proposed design for resonant mode shapes, eigenfrequencies, to study the stresses and displacement in the structure and verify the analytical model. Initially, the modal analysis is performed to find eigenfrequencies and the different mode shapes of the tuning fork. All simulations were carried out by using COMSOL Multiphysics 5.3 structural mechanical module. A 3D model of quartz tuning fork with flexible base was created by COMSOL Multiphysics 5.3. The finite element method is briefly explained as following: -

4.1 Boundary Condition

To perform any FEM simulation, one must define some boundary condition, initial condition and some fixed or free constraints. Following are the boundary condition defined in FEM for the proposed design.

1) The base support of the tuning fork type TF-A, TF-B and TF-C as shown in Figure 2.1, in chapter 2, are considered as fixed constraints (having zero displacement in all axes).
2) The electrical conditions are not applied to the model.

The same boundary condition was considered while developing the analytical model. During computation, the software automatically applies the electrical load to the model and the obtained results are found in Figure 4.1. There is no other electrical and mechanical load applied to the model.

4.1.1 Material Properties

To make the geometric model as realistic as possible, special care was taken to specify the material properties such as Young's modulus, Poisson's ratio and density of quartz respectively. As these required special knowledges of the relevant material. These material properties are listed in Table. 1 and were employed by selecting the entries from materials library of simulation software and calculated the inphase and antiphase eigenfrequencies of tuning fork.

Table 1: Material properties used in FEM Based simulations.

Property	Value	Unit
Density	2650	$kg.m^{-3}$
Poisson's ratio	0.7	
Young's modulus	78.7	*GPa*

4.1.2 Geometrical Dimensions

The 3D model of tuning fork type TF-C with flexible base is design in COMSOL Multiphysics 5.3. The Dimensions of the proposed quartz tuning fork model and inter-tines coupling are enlisted in Table 2 & 3. The *L, W, T* and l_h, w_h, t_h represents the length, width, thickness of tuning fork and coupling hinges respectively. The geometry of substrate is l_b=350, w_b=230, t_b=350.

Table 2: Enlisted the relevant geometric parameters used to design the quartz tuning fork and coupling hinges between tines.

TF-C	Dimensions (µm)	Coupling hinges	Dimensions (µm)
L	3200	l_h	330
W	125	t_h	30
T	235	w_h	230

Table 3: The dimension used for tuning fork type TF-A, type TF-B and type TF-C.

	TF-A (Exp)	TF-A (Sim)	TF-B (Exp)	TF-B (Sim)	TF-C (Sim)
L (µm)	3200	3200	2500	2500	3200
W (µm)	125	125	100	100	125
T (µm)	235	235	235	235	235
Prong spacing *(µm)*	--	200	--	150	445

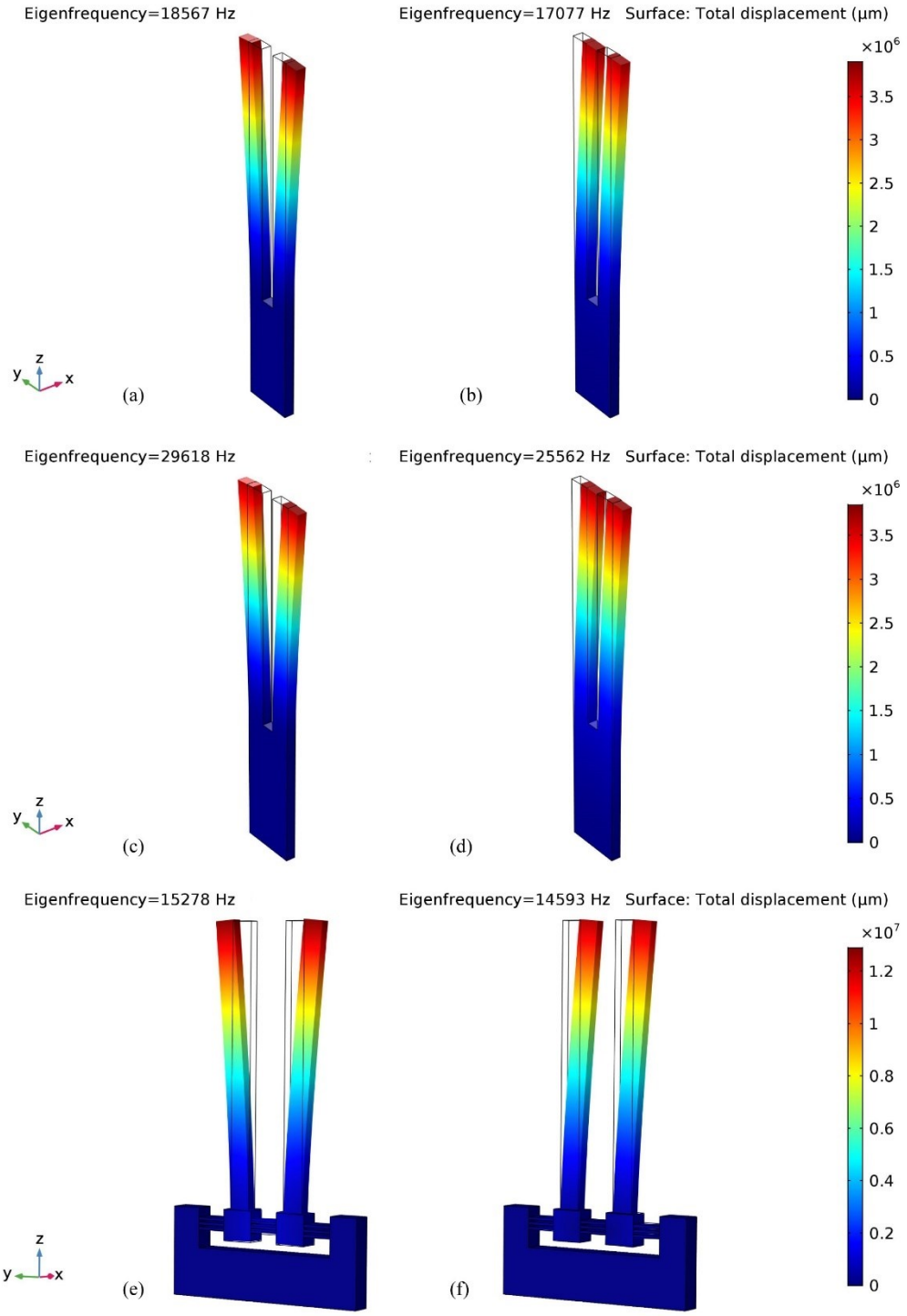

Figure 4.1: Simulation results. (a) & (b) Standard tuning fork type TF-A with antiphase and inphase mode shapes and eigenfrequencies. (c) & (d) Standard tuning fork type TF-B with antiphase and inphase mode shapes and eigenfrequencies. (e) & (f) New designed tuning fork type TF-C with antiphase and inphase mode shapes and eigenfrequencies.

The Figure 4.1 (a) and (b) shows the antiphase and inphase modes of TF-A, (c) and (d) shows the antiphase and inphase modes of TF-B, (e) and (f) shows the antiphase and inphase modes of TF-C respectively. As the coupling spring constant (k_c) for tuning fork type TF-C is lower than TF-A and TF-B because of flexible base. Therefore, tines of TF-C vibrate with higher amplitude and closely spaced eigenfrequencies of two resonance modes than tuning fork type TF-A and TF-B as shown in Figure 4.1.

4.2 Comparison of the Obtained Results by Simulation with the Standard Model

In this paper, we used (3.17) and (3.18) for the eigenfrequencies obtained from simulations. Table 4 gives the comparison between the obtained values of effective spring constant (k_{eff}), coupling spring constant (k_c) for tuning fork type-A, type-B given in [64] and type-C (new design), measured by experimental and simulation methods.

Table 4: Comparison between different tuning fork models using simulation and experimental methods [64].

	TF-A (exp)	**TF-A (sim)**	**TF-B (exp)**	**TF-B (sim)**	**TF-C (sim)**
$f^{inphase}$ ***(Hz)***	18255	17077	27800	25562	14593
$f^{antiphase}$***(Hz)***	20000	18567	32766	29618	15278
L (μm)	3200	3200	2500	2500	3200
W (μm)	125	125	100	100	125
T (μm)	235	235	235	235	235
Prong spacing *(μm)*	--	200	--	150	445
$k\ (Nm^{-1})$	974	974	1634	1634	974
$k_c\ (Nm^{-1})$	98	88.7	318	279.8	46.8
$k_{eff}\ (Nm^{-1})$	2338	2302.8	4540	4387.4	2135.2

There is slight difference between coupling spring constant (k_c) and effective spring constant (k_{eff}) values determined by experimental and simulation methods. The difference in coupling spring constant (k_c) for TF-A is 9.3 Nm^{-1} and for TF-B is 38.2 Nm^{-1} as manifested by Table. 1. Similarly, there is small difference between effective spring constant (k_{eff}) calculated by experimental and simulation methods. The difference in effective spring constant (k_{eff}) for TF-A is 35.2 Nm^{-1} and for TF-B is 152.6 Nm^{-1}. We have calculated the coupling spring constant (k_c) and effective spring constant (k_{eff}) for quartz tuning fork with flexible base proposed, by equations illustrated in the literature [64], and obtained results are shown in Table. 4.

4.3 Conclusion

In this chapter, the finite element analysis of QTF is briefly described. Finite Element Analysis is important to simulate the proposed design for resonant mode shapes, eigenfrequencies, to study the stresses and displacement in the structure and verify the analytical model. In FEM, modal analysis is performed by specifying boundary condition, material properties and geometric properties to determine eigenfrequencies and the different mode shapes of the tuning fork. For simulations and 3D model of quartz tuning fork COMSOL Multiphysics 5.3 structural mechanical module were used. The FEM image and comparison between results obtained by simulation and experiments for effective spring constant (k_{eff}), coupling spring constant (k_c) for tuning fork TF-A, TF-B and T F-C (new design) are also discussed.

Chapter 5: Impact of Inter Tine Coupling on the Spring Constant of the Quartz Tuning Fork

We have investigated the dimensional impact of coupling hinges on the spring constant of quartz tuning fork. The eigenfrequencies, effective spring constant (k_{eff}), coupling spring constant (k_c) and sensitivity are determined by varying length (t_h), width (w_h) and thickness (t_h). The results are shown by following figures.

5.1 Background

There are many factors which contributes to damping losses for example medium surrounding the tines [10], support and anchor [11], thermoelastic [12] and surface of tines [13]. Support is one of main contributing factor to damping loss that effect the TF sensitivity and quality (Q) factor. The tuning fork with coupled tines has higher quality (Q) factor than single cantilever beam. When single cantilever beam is made to oscillate at specified frequency, the energy waves induced in beam propagates to the fixed and stiff support causing high energy loss as well as attenuation in quality (Q) factor. In quartz tuning fork with identical prongs, the generated energy waves in both prongs moves toward support and mostly utilized for vibration of each tines through base which acts like coupling spring. Therefore, coupling between tines is highly important for reducing damping losses in the tuning fork. In this research work, we propose a new design where parallel hinges of quartz act as coupling spring between the tines of the quartz tuning fork and investigate the dimensional impact of coupling hinges on the spring constant of QTF. The results are shown by following figures.

5.2 Results and Discussion

The Figure 5.1 shows relationship between coupling hinges geometry and eigenfrequencies of tuning fork. The eigenfrequencies are inversely proportional to the length (l_h) of coupling hinges as illustrated in Figure 5.1. As length (l_h) of hinges increases, the magnitudes of inphase and antiphase eigenfrequencies decrease. The inphase frequency decreases more rapidly than antiphase frequency.

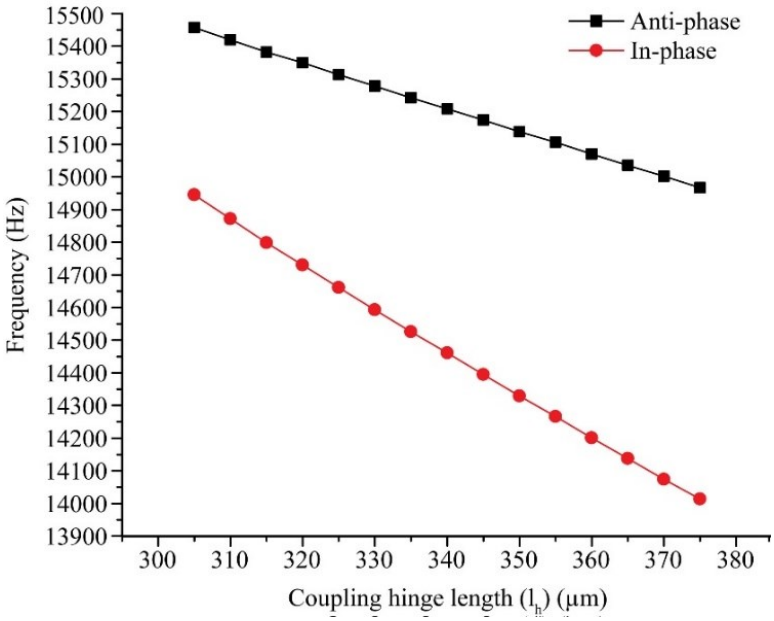

Figure 5.1: Impact of coupling hinges length (l_h) on inphase and antiphase eigenfrequencies of the tuning fork.

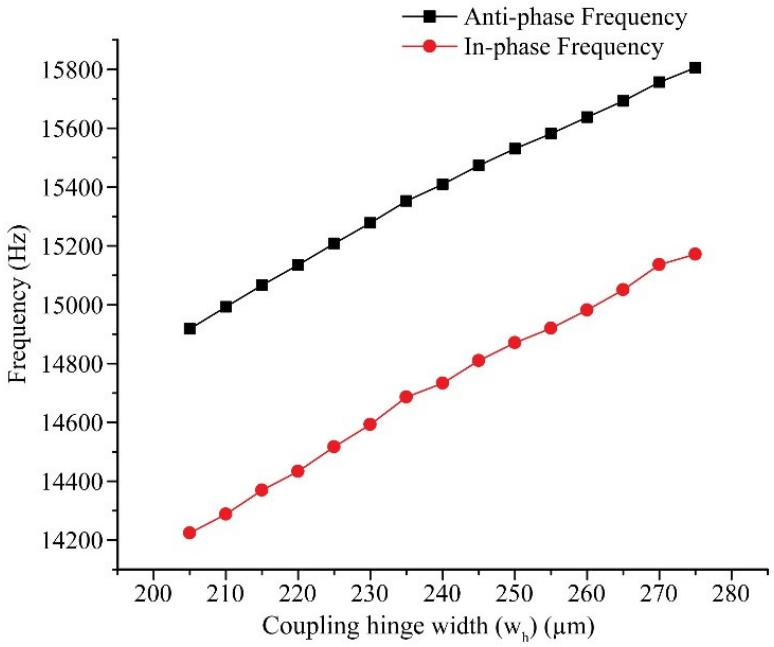

Figure 5.2: Impact of coupling hinges width (w_h) on inphase and antiphase eigenfrequencies of the tuning fork.

The relation between width (w_h) of coupling hinges and eigenfrequencies are shown in Figure 5.2. With the increasing width (w_h), the magnitudes of both eigenfrequencies also increases.

Similarly, the Figure 5.3 shows the effect of increasing coupling hinges thickness (t_h) on eigenfrequencies of tuning fork. With the increase in thickness (t_h), the inphase and antiphase eigenfrequencies also increases. The increase in thickness (t_h) of coupling hinges, lowers the coupling spring constant (k_c) as shown in Figure 5.4 (c). From equation (3.16), it is manifested that by attenuation in coupling spring constant (k_c), the separation between magnitudes of both the eigenfrequencies reduces as depicted in Figure 5.3.

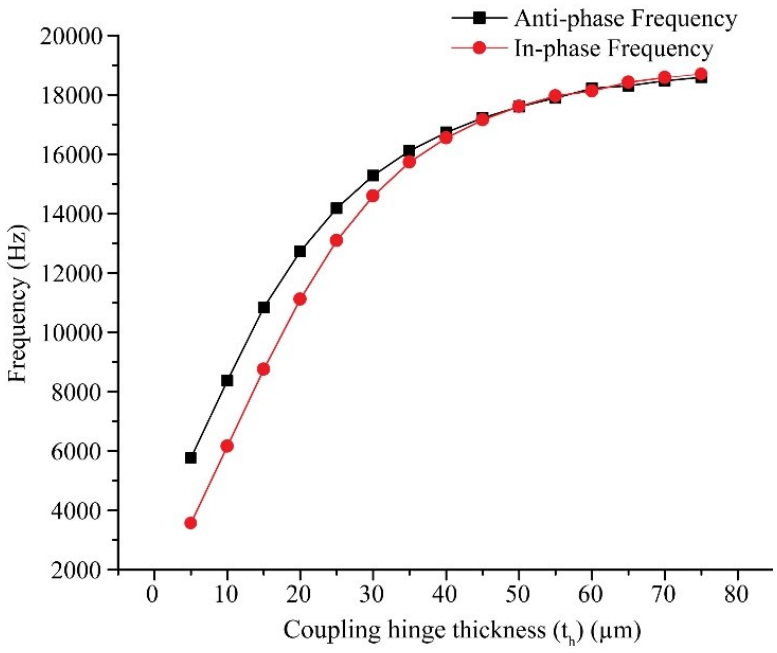

Figure 5.3: Shows the influence of coupling hinges thickness (t_h) on the eigenfrequencies.

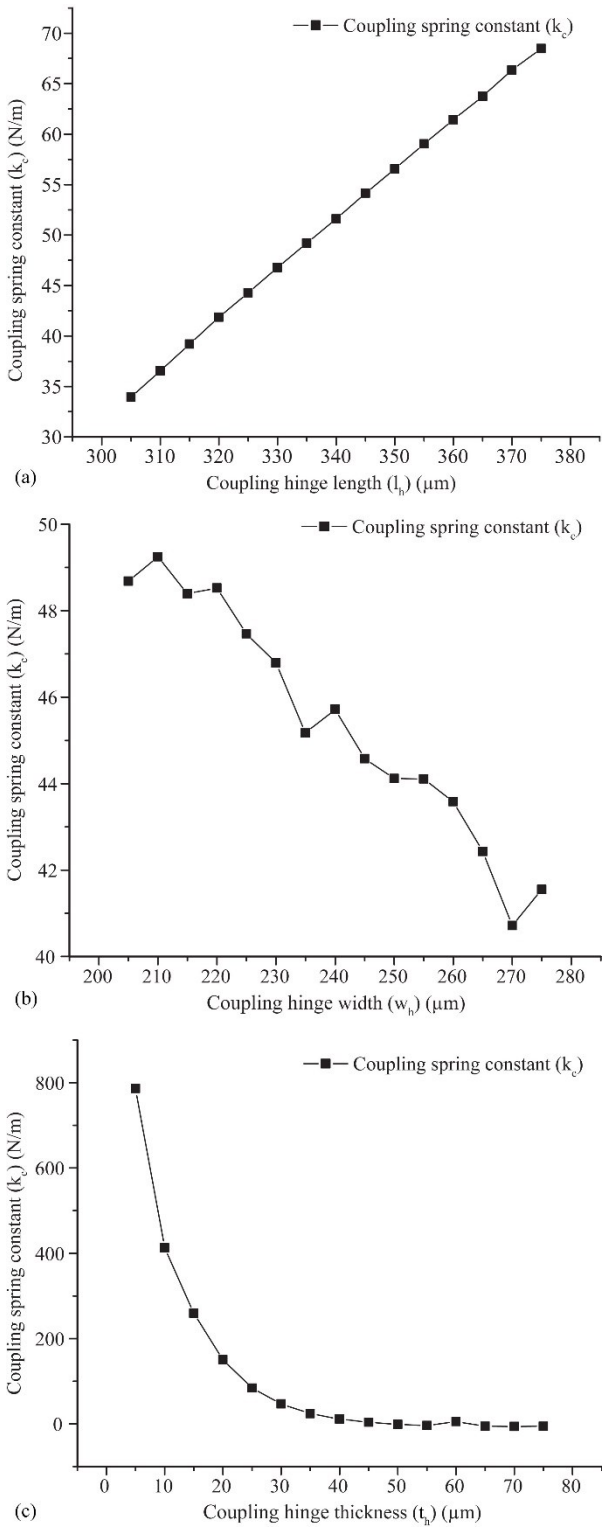

Figure 5.4 Shows the influence of coupling hinges on coupling spring constant (k_c). (a) Impact of hinges length (l_h) on coupling spring constant (k_c). (b) Impact of hinges width (w_h) on coupling spring constant (k_c). (c) Impact of hinges thickness (t_h) on coupling spring constant (k_c).

The Figure 5.4 (a) illustrates the linear relationship between length (l_h) of coupling hinges and coupling spring constant (k_c). As the length (l_h) increases, the coupling spring constant (k_c) also increase linearly. The influence of increasing coupling hinges width (w_h) on coupling spring constant (k_c) is shown in Figure 5.4 (b). With the increasing width (w_h), coupling spring constant (k_c) reduces. The Figure 5.4 (c) shows the decreasing trend in coupling spring constant (k_c) with the increase of hinges thickness (t_h). In the beginning, coupling spring constant (k_c) reduces vary rapidly with the increase in thickness (t_h) (from 5 µm to 30 µm) but later the reduction rate is lower because of closely spaced eigenfrequencies.

As the quartz tuning fork is fundamentally a cantilever beam, therefore similar trends in relation between effective spring constant (k_{eff}) and geometry of coupling hinges (l_h, w_h, t_h) are shown in Figure 5.5.

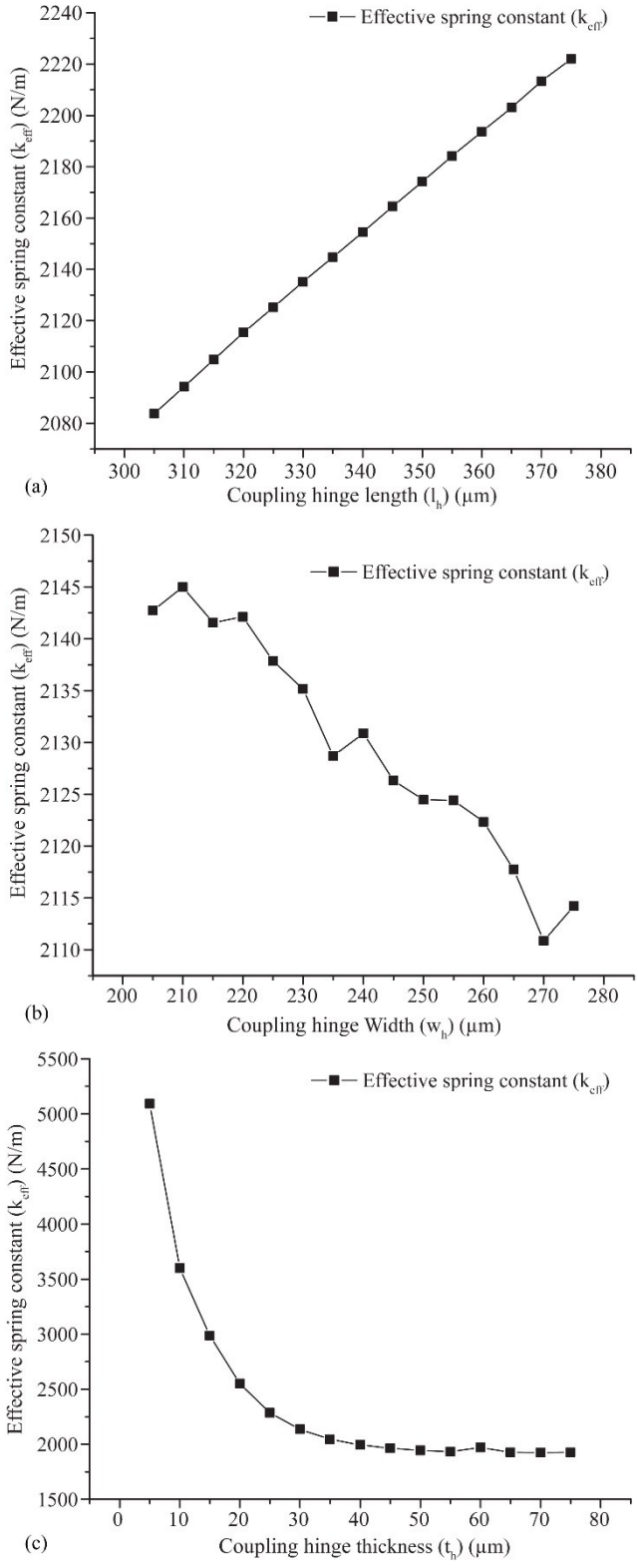

Figure 5.5 Shows the relation between coupling hinges geometry (l_h, w_h, t_h) and effective spring constant (k_{eff}).

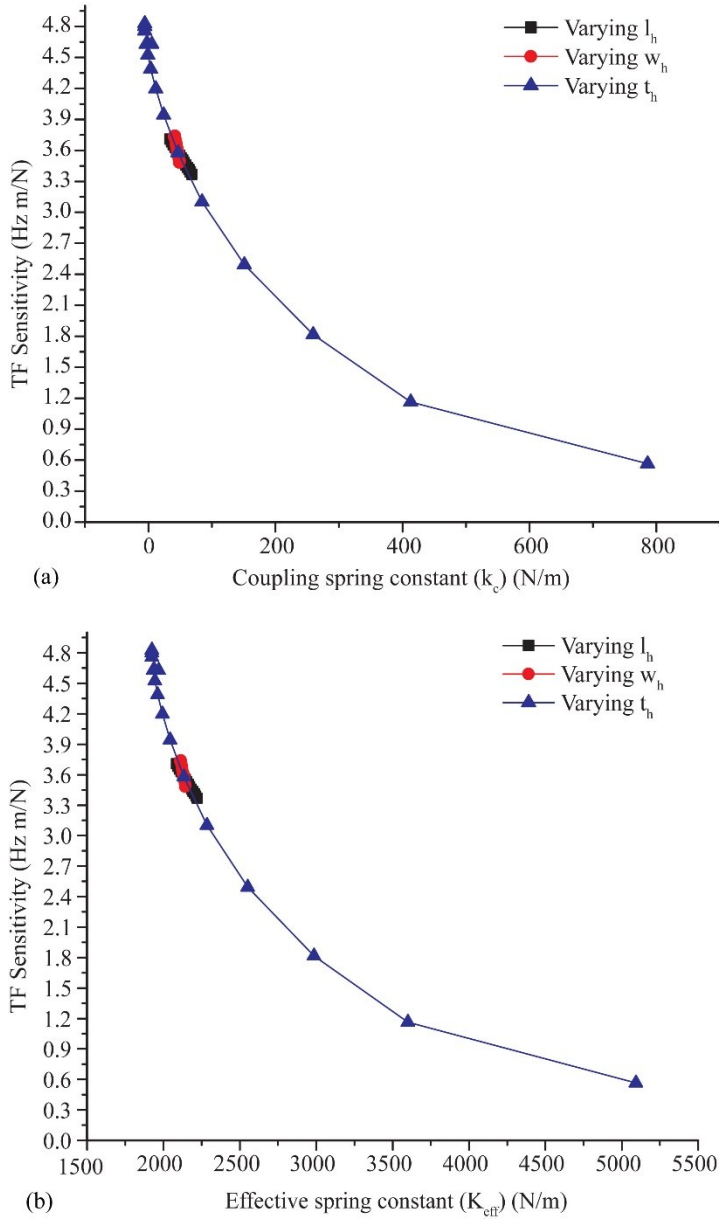

Figure 5.6 (a) Shows relation between TF sensitivity and coupling spring constant (k_c). (b) Relation between TF sensitivity and effective spring constant (k_{eff}).

The Figure 5.6 (a) illustrates the relationship between coupling spring constant (k_c) and tuning fork sensitivity. The relation between effective spring constant (k_{eff}) and tuning fork sensitivity are shown in Figure 5.6 (b). The Figure (5.4 & 5.5) shows that coupling spring constant (k_c) and effective spring constant (k_{eff}) varies in similar fashion with the changing geometry of coupling hinges. The tuning fork sensor sensitivity can be found as [64].

$$\alpha = \frac{f_{anti-phase}}{2k_{eff}} \tag{5.1}$$

From equation (1.1), we can express the relation between TF sensitivity and coupling spring constant (k_c) as,

$$\alpha = \frac{f_{anti-phase}}{4[k + 2k_c]} \tag{5.2}$$

Equations (5.1) and (5.2) shows that by decreasing coupling spring constant (k_c) and effective spring constant (k_{eff}), the TF sensitivity can be improved. When coupling spring constant (k_c) is decreases, the effective spring constant (k_{eff}) will also decrease while improving TF sensitivity. To have a lower coupling spring constant (k_c), we need coupling hinges with shorter length (l_h) and relatively higher width (w_h) and thickness (t_h).

From Figure 5.6, it is depicted that as coupling spring constant (k_c) and effective spring constant (k_{eff}) decreases, the TF sensitivity increase. If we increase coupling hinges thickness (t_h) within some limits, then relatively coupling spring constant (k_c) decreases.

5.3 Future Work

This work will facilitate the researcher to design and optimize the quartz tuning fork in order to improve quality (Q) factor and sensitivity to be used for the specific application having cantilever beam as basic element such Atomic Force Microscopy (AFM).

5.4 Conclusion

In this chapter, the influence of coupling hinges by varying its length (t_h), width (w_h) and thickness (t_h) on the eigenfrequencies, effective spring constant (k_{eff}), coupling spring constant (k_c) and sensitivity are discussed with figures. The figures show that by changing geometry of coupling hinges, the coupling constant (k_c) as well as effective constant (k_{eff}) reduces which can significantly improves the TF sensitivity. Lastly, the significance of this research work in future are also described.

Chapter 6: Conclusion

The quartz tuning fork (QTF) is an excellent mechanical resonator consisting of two prongs. It is widely used as a time keeping element in watches and telecommunication industry due to its high frequency stability. For using QTF as a force sensor in atomic force microscopy, high quality (Q) factor, high force sensitivity and relatively low spring constant are desirable properties.

In this research work, the design of quartz tuning fork (QTF) with flexible base is proposed. The new design has flexible coupling hinge structures between two prongs of tuning fork. For the performance analysis of QTF, the analytical model is developed and furthermore the FEM simulation are done. Finite Element Analysis is important to simulate the proposed design for resonant mode shapes, eigenfrequencies, to study the stresses and displacement in the structure and verify the analytical model. The tuning fork with coupled tines has higher quality (Q) factor than single cantilever beam. In the vibration of single cantilever beam, the energy waves induced in beam propagates to the fixed and stiff support causing high energy loss as well as attenuation in quality (Q) factor. In quartz tuning fork with identical prongs, the generated energy waves in both prongs moves toward support and mostly utilized for vibration of each tines through base which acts like coupling spring. Therefore, coupling between tines is highly important for reducing damping losses in the tuning fork. In the new design of QTF with flexible base, parallel hinges of quartz act as coupling spring between the tines of the quartz tuning fork. We have investigated the influence of inter-tine coupling of quartz tuning fork by varying its length (t_h), width (w_h) and thickness (t_h) on its eigenfrequencies, effective spring constant (k_{eff}) and sensitivity. The analytical and simulation results show that by changing geometry of coupling hinges, we can reduce the coupling constant (k_c) as well as effective constant (k_{eff}) which can significantly enhance the TF sensitivity. For lower coupling spring constant (k_c), we need coupling hinges with shorter length (l_h) and relatively higher width (w_h) and thickness (t_h).

References

[1] D. Hussain, Y. Wen, H. Zhang, J. Song, and H. Xie, "Atomic Force Microscopy Sidewall Imaging with a Quartz Tuning Fork Force Sensor," *Sensors,* vol. 18, no. 1, 2018.

[2] C. Yuan-Liu, X. Yanhao, S. Yuki, M. Hiraku, and G. Wei, "High quality-factor quartz tuning fork glass probe used in tapping mode atomic force microscopy for surface profile measurement," *Measurement Science and Technology,* vol. 29, no. 6, p. 065014, 2018.

[3] D. Ebeling, Q. Zhong, S. Ahles, L. Chi, H. A. Wegner, and A. Schirmeisen, "Chemical bond imaging using higher eigenmodes of tuning fork sensors in atomic force microscopy," *Applied Physics Letters,* vol. 110, no. 18, p. 183102, 2017/05/01 2017.

[4] H. Mönig *et al.*, "Quantitative assessment of intermolecular interactions by atomic force microscopy imaging using copper oxide tips," *Nature Nanotechnology,* vol. 13, no. 5, pp. 371-375, 2018/05/01 2018.

[5] A. Juan Camilo, P.-M. Jérôme, T. François, X. Hui, H. Sinan, and R. Stéphane, "Gentle and fast atomic force microscopy with a piezoelectric scanning probe for nanorobotics applications," *Nanotechnology,* vol. 24, no. 6, p. 065502, 2013.

[6] J. Abrahamians, B. Sauvet, J. Polesel-Maris, R. Braive, and S. Régnier, "Robotic in situ stiffness cartography of InP membranes by dynamic force sensing," in *2013 IEEE/RSJ International Conference on Intelligent Robots and Systems*, 2013, pp. 1016-1021.

[7] P. Patimisco *et al.*, "Loss Mechanisms Determining the Quality Factors in Quartz Tuning Forks Vibrating at the Fundamental and First Overtone Modes," *IEEE Transactions on Ultrasonics, Ferroelectrics, and Frequency Control,* vol. 65, no. 10, pp. 1951-1957, 2018.

[8] H. T. Wei, C. Y. Hsu, and S. J. Chen, "Research on miniature quartz tuning fork with quality factor," in *2014 9th International Microsystems, Packaging, Assembly and Circuits Technology Conference (IMPACT)*, 2014, pp. 494-497.

[9] P. Patimisco *et al.*, "Analysis of the electro-elastic properties of custom quartz tuning forks for optoacoustic gas sensing," *Sensors and Actuators B: Chemical,* vol. 227, pp. 539-546, 2016/05/01/ 2016.

[10] H. Hosaka, K. Itao, and S. Kuroda, "Damping characteristics of beam-shaped micro-oscillators," *Sensors and Actuators A: Physical,* vol. 49, no. 1, pp. 87-95, 1995/06/01/ 1995.

[11] Z. Hao, A. Erbil, and F. Ayazi, "An analytical model for support loss in micromachined beam resonators with in-plane flexural vibrations," *Sensors and Actuators A: Physical,* vol. 109, no. 1, pp. 156-164, 2003/12/01/ 2003.

[12] C. Zener, "Internal Friction in Solids II. General Theory of Thermoelastic Internal Friction," *Physical Review,* vol. 53, no. 1, pp. 90-99, 01/01/ 1938.

[13] J. Yang, T. Ono, and M. Esashi, "Surface effects and high quality factors in ultrathin single-crystal silicon cantilevers," *Applied Physics Letters,* vol. 77, no. 23, pp. 3860-3862, 2000/12/04 2000.

[14] T. D. Rossing, D. A. Russell, and D. E. Brown, "On the acoustics of tuning forks," *American Journal of Physics,* vol. 60, no. 7, pp. 620-626, 1992/07/01 1992.

[15] R. L. Scott, "Precise electronic aid to musical instrument tuning," ed: Google Patents, 1991.

[16] H. F. Olson and H. J. T. J. o. t. A. S. o. A. Belar, "Electronic music synthesizer," vol. 27, no. 3, pp. 595-612, 1955.

[17] M. Ren, E. S. Forzani, and N. J. A. c. Tao, "Chemical sensor based on microfabricated wristwatch tuning forks," vol. 77, no. 9, pp. 2700-2707, 2005.

[18] Y. Qin, "Interaction force microscopy based on quartz tuning fork force sensor," Purdue University, 2007.

[19] J. A. Babbitt, "LXXXII. Conservative Treatment in Diseases of the Ear," *Annals of Otology, Rhinology & Laryngology,* vol. 43, no. 4, pp. 1001-1008, 1934/12/01 1934.

[20] G. Miller, D. M. Oster, and C. G. Crampton, "Electronic tuning device," ed: Google Patents, 1995.

[21] F. Kitamura, J. Sakata, and H. Tanaya, "Vibrating piece, vibrator, oscillator, and electronic equipment," ed: Google Patents, 2003.

[22] C. F. Clifford, "Tuning fork with frequency adjustment," ed: Google Patents, 1970.

[23] W.-P. Kao and S.-P. Yang, "Electric plug for use in a mobile electronic apparatus," ed: Google Patents, 2005.

[24] J. Abrahamians, B. Sauvet, J. Polesel-Maris, R. Braive, and S. Régnier, "A Nanorobotic System for In Situ Stiffness Measurements on Membranes," *IEEE Transactions on Robotics,* vol. 30, no. 1, pp. 119-124, 2014.

[25] J. C. Acosta, G. Hwang, F. Thoyer, J. Polesel-Maris, and S. Régnier, "Tuning fork based in situ SEM nanorobotic manipulation system for wide range mechanical characterization of ultra flexible nanostructures," in *2010 IEEE/RSJ International Conference on Intelligent Robots and Systems*, 2010, pp. 5780-5785.

[26] J. Toledo *et al.*, "Application of quartz tuning forks and extensional microresonators for viscosity and density measurements in oil/fuel mixtures," *Microsystem Technologies,* vol. 20, no. 4, pp. 945-953, 2014/04/01 2014.

[27] G. Binnig, H. Rohrer, C. Gerber, and E. Weibel, "Surface Studies by Scanning Tunneling Microscopy," *Physical Review Letters,* vol. 49, no. 1, pp. 57-61, 07/05/ 1982.

[28] G. Binnig and H. Rohrer, "Scanning tunneling microscopy---from birth to adolescence," *Reviews of Modern Physics,* vol. 59, no. 3, pp. 615-625, 07/01/ 1987.

[29] R. Wiesendanger and W. Roland, *Scanning probe microscopy and spectroscopy: methods and applications*. Cambridge university press, 1994.

[30] J. J. A. M. Loos, "The art of SPM: Scanning probe microscopy in materials science," vol. 17, no. 15, pp. 1821-1833, 2005.

[31] K. D. J. M. S. Jandt and E. R. Reports, "Developments and perspectives of scanning probe microscopy (SPM) on organic materials systems," vol. 21, no. 5-6, pp. 221-295, 1998.

[32] J. Loos, "The Art of SPM: Scanning Probe Microscopy in Materials Science," *Advanced Materials,* vol. 17, no. 15, pp. 1821-1833, 2005/08/04 2005.

[33] G. Binnig and C. J. P. R. L. Quate, "Gerber Ch. Atomisk kraftmikroskop," vol. 56, no. 9, pp. 930-933, 1986.

[34] G. Binnig, C. F. Quate, and C. Gerber, "Atomic Force Microscope," *Physical Review Letters,* vol. 56, no. 9, pp. 930-933, 03/03/ 1986.

[35] G. Binnig, C. Gerber, E. Stoll, T. R. Albrecht, and C. F. Quate, "Atomic Resolution with Atomic Force Microscope," *Europhysics Letters (EPL),* vol. 3, no. 12, pp. 1281-1286, 1987/06/15 1987.

[36] U. Hartmann, "Theory of magnetic force microscopy," *Journal of Vacuum Science & Technology A,* vol. 8, no. 1, pp. 411-415, 1990/01/01 1990.

[37] B. D. Terris, J. E. Stern, D. Rugar, and H. J. Mamin, "Contact electrification using force microscopy," *Physical Review Letters,* vol. 63, no. 24, pp. 2669-2672, 12/11/ 1989.

[38] E. Betzig, J. K. Trautman, T. D. Harris, J. S. Weiner, and R. L. Kostelak, "Breaking the Diffraction Barrier: Optical Microscopy on a Nanometric Scale," *Science,* vol. 251, no. 5000, p. 1468, 1991.

[39] R. Erlandsson, L. Olsson, and P. Mårtensson, "Inequivalent atoms and imaging mechanisms in ac-mode atomic-force microscopy of Si(111)7\ifmmode\times\else\texttimes\fi{}7," *Physical Review B,* vol. 54, no. 12, pp. R8309-R8312, 09/15/ 1996.

[40] T. R. Albrecht and C. F. Quate, "Atomic resolution imaging of a nonconductor by atomic force microscopy," *Journal of Applied Physics,* vol. 62, no. 7, pp. 2599-2602, 1987/10/01 1987.

[41] T. R. Albrecht and C. F. Quate, "Atomic resolution with the atomic force microscope on conductors and nonconductors," *Journal of Vacuum Science & Technology A,* vol. 6, no. 2, pp. 271-274, 1988/03/01 1988.

[42] U. Hartmann, "Theory of van der Waals microscopy," *Journal of Vacuum Science & Technology B: Microelectronics and Nanometer Structures Processing, Measurement, and Phenomena,* vol. 9, no. 2, pp. 465-469, 1991/03/01 1991.

[43] F. J. J. R. o. m. p. Giessibl, "Advances in atomic force microscopy," vol. 75, no. 3, p. 949, 2003.

[44] P. De Pablo, J. Colchero, J. Gomez-Herrero, and A. J. A. P. L. Baro, "Jumping mode scanning force microscopy," vol. 73, no. 22, pp. 3300-3302, 1998.

[45] H.-J. Butt, B. Cappella, and M. Kappl, "Force measurements with the atomic force microscope: Technique, interpretation and applications," *Surface Science Reports,* vol. 59, no. 1, pp. 1-152, 2005/10/01/ 2005.

[46] W. A. Ducker, T. J. Senden, and R. M. Pashley, "Direct measurement of colloidal forces using an atomic force microscope," *Nature,* vol. 353, no. 6341, pp. 239-241, 1991/09/01 1991.

[47] Y. F. Dufrêne *et al.*, "Imaging modes of atomic force microscopy for application in molecular and cell biology," *Nature Nanotechnology,* Review Article vol. 12, p. 295, 04/06/online 2017.

[48] M. Radmacher, R. W. Tillamnn, M. Fritz, and H. E. Gaub, "From molecules to cells: imaging soft samples with the atomic force microscope," *Science,* vol. 257, no. 5078, p. 1900, 1992.

[49] T. Junno, K. Deppert, L. Montelius, and L. Samuelson, "Controlled manipulation of nanoparticles with an atomic force microscope," *Applied Physics Letters,* vol. 66, no. 26, pp. 3627-3629, 1995/06/26 1995.

[50] O. Custance, R. Perez, and S. Morita, "Atomic force microscopy as a tool for atom manipulation," *Nature Nanotechnology,* Review Article vol. 4, p. 803, 12/06/online 2009.

[51] R. Lal and S. A. John, "Biological applications of atomic force microscopy," *American Journal of Physiology-Cell Physiology,* vol. 266, no. 1, pp. C1-C21, 1994/01/01 1994.

[52] L. Wilson, P. T. Matsudaira, B. P. Jena, and J. H. Horber, *Atomic force microscopy in cell biology*. Academic Press, 2002.

[53] H. Liu, S. Fu, J. Zhu, H. Li, H. J. E. Zhan, and m. technology, "Visualization of enzymatic hydrolysis of cellulose using AFM phase imaging," vol. 45, no. 4, pp. 274-281, 2009.

[54] M. Firtel, G. Henderson, and I. J. U. Sokolov, "Nanosurgery: observation of peptidoglycan strands in Lactobacillus helveticus cell walls," vol. 101, no. 2-4, pp. 105-109, 2004.

[55] D. J. J. B. Muller, "AFM: a nanotool in membrane biology," vol. 47, no. 31, pp. 7986-7998, 2008.

[56] C. R. Valois, L. P. Silva, R. B. Azevedo, E. D. J. O. S. Costa Jr, Oral Medicine, Oral Pathology, Oral Radiology,, and Endodontology, "Atomic force microscopy study of gutta-percha cone topography," vol. 98, no. 2, pp. 250-255, 2004.

[57] J. A. Harley, "Advances in piezoresistive probes for atomic force microscopy," Stanford University, 2000.

[58] J. O. Jacobsen, G. Chen, L. L. Howell, and S. P. Magleby, "Lamina Emergent Torsional (LET) Joint," *Mechanism and Machine Theory,* vol. 44, no. 11, pp. 2098-2109, 2009/11/01/ 2009.

[59] A. Naber, "The tuning fork as sensor for dynamic force distance control in scanning near-field optical microscopy," *Journal of Microscopy,* vol. 194, no. 2-3, pp. 307-310, 1999/05/01 1999.

[60] B. P. Ng, Y. Zhang, S. Wei Kok, and Y. Chai Soh, "Improve performance of scanning probe microscopy by balancing tuning fork prongs," *Ultramicroscopy,* vol. 109, no. 4, pp. 291-5, Mar 2009.

[61] R. D. Grober *et al.*, "Fundamental limits to force detection using quartz tuning forks," *Review of Scientific Instruments,* vol. 71, no. 7, pp. 2776-2780, 2000/07/01 2000.

[62] K. Karrai and R. D. Grober, "Piezoelectric tip-sample distance control for near field optical microscopes," *Applied Physics Letters,* vol. 66, no. 14, pp. 1842-1844, 1995/04/03 1995.

[63] W. H. J. Rensen, N. F. van Hulst, A. G. T. Ruiter, and P. E. West, "Atomic steps with tuning-fork-based noncontact atomic force microscopy," *Applied Physics Letters,* vol. 75, no. 11, pp. 1640-1642, 1999/09/13 1999.

[64] A. Castellanos-Gomez, N. Agraït, and G. Rubio-Bollinger, "Dynamics of quartz tuning fork force sensors used in scanning probe microscopy," *Nanotechnology,* vol. 20, no. 21, p. 215502, 2009.

[65] K. Karrai and R. D. Grober, "Piezoelectric tip-sample distance control for near field optical microscopes," vol. 66, no. 14, pp. 1842-1844, 1995.

Completion Certificate

It is certified that the contents of thesis document titled "***Investigation of Quartz Tuning Fork's Dimensional Impact on its Dynamics and Resonance Frequency***" submitted by NS Sajid Parveez, Registration No. 00000172262 have been found satisfactory in all respects as per the requirements of Main Office, NUST (Exam branch).

Supervisor: _____

Dr. Danish Hussain

Date: ____ June, 2019